Department of Physics and Astronomy
University of Heidelberg

Bachelor Thesis in Physics
submitted by

Stephan Friedrich Stiefelmaier

born in Kirchheim unter Teck (Germany)

2012

Extrapolation Of D Meson Cross Sections

This Bachelor Thesis has been carried out by Stephan Stiefelmaier at the
Physikalisches Institut of University of Heidelberg
under the supervision of
Dr. Kai Schweda

Abstract

Within this thesis a program was developed in object-oriented C++, that extrapolates the visible cross sections of D mesons measured in the ALICE experiment to the full phase space, using results from the pQCD framework FONLL for calculation of the extrapolation factors. From the total D meson production cross section the total charm quark production cross section is determined. Moreover, P_v, the fraction of $c\bar{d}$ mesons produced in vector state is calculated. Comparison was made to existing results from an older, outdated code. Central values were correctly reproduced. However, diffrences in the assigned uncertainties were traced to faulty error propagation in the old code.

Kurzdarstellung

Thema dieser Arbeit war die Entwicklung eines Computerprogramms, welches die im ALICE Experiment gemessenen sichtbaren Wirkungsquerschnitte von D Mesonen auf den ganzen kinematischen Phasenraum extrapoliert. Die Extrapolationsfaktoren werden dabei mithilfe von Ergebnissen des pQCD frameworks FONLL berechnet. Aus dem totalen D Meson Produktionswirkungsquerschnitt wird der totale Charm Quark Produktionswirkungsquerschnitt berechnet. Außerdem wird P_v, der Anteil von $c\bar{d}$ Mesonen, die in einem Verktorzustand produziert werden, berechnet. Die Ergebnisse wurden mit denen eines Vorgängerrogramms verglichen. Dabei stellte sich heraus, dass die Berechung mehrerer Unsicherheiten in dem Vorgängerprogramm fehlerhaft implementiert ist.

Contents

1 Introduction

The measurement of charm quark production cross sections in proton-proton collisions constitutes a fundamental test of calculations in pertubative QCD. Amongst others, such measurements are performed in the ALICE experiment at the Large Hadron Collider (LHC) at CERN, where proton-proton collisions at center of mass energies of up to $\sqrt{s} = 7\,\mathrm{TeV}$ are taking place. The hereby produced charm quarks and anti-quarks cannot be detected directly as they hadronise into hadrons soon after their production. Most of the charm (roughly 90 %) hadronises into D mesons (particles that consist of a charm quark (or anti-quark) and an anti-quark (or quark)). The study of D mesons therefore allows for drawing conclusions on the production of charm quarks. Due to their large mass, the D mesons decay before they can reach the detectors. Therefore, one exploits their decays into kaons and pions. As the detectors see particles only in certain p_t and rapidity ranges, the cross sections observed by the detectors are called visible cross sections - meaning that the total production cross section of the the particle species being investigated might be larger.

Within this thesis, a program was written that extrapolates the visible cross sections of D mesons to the full phase space. The hereby obtained values are the total production cross sections of the D mesons. The total charm production cross section is then computed from the total production cross sections of the D mesons. Moreover, a closer look on the process of hadronisation is taken by examinig how many D^+ mesons are produced in a vector state in comparison to the total number of produced D^+ mesons.

Before this thesis, these calculations were performed using another, already existing program. This program had once been written for the purpose of providing results within short time. The disadvantage of this program is that its source-code is hard to maintain. Therefore it was important, that the newly developed program would have a well-arranged source-code being easy to maintain.

A major part of this thesis was to compare the values produced by the new program with the already existing values. The actual numbers of the cross sections were reproduced, however, it turned out that there were some bugs in the old code concernig the calculation of uncertainties.

After the process of checking and comparing had been completed, the developed program was upgraded and used to extrapolate the cross section of the D_s^+ meson. This meson has only recently been analysed within the ALICE collaboration and was therefore not integrated in the already existing program.

This thesis is organized as follows:
Section 2 gives a short summary of the regarded processes within the standard modell. Moreover, some basic information about the pQCD framework FONLL that provided the theoretical spectra which were used to compute the extrapolation factors is presented. In Section 3 all extrapolations and calculations performed by the program are described. To achieve a more fluent text most of the equations that describe the propagation of uncertainties have been moved to the Appendix. In Section 4 the results produced by the developed program are presented along with the diffrences and bugs found in the existing code. In Section 5 the last carried out implementation of the D_s^+ meson is presented. In Section 6 a short summary is given.

2 Theoretical Background

2.1 Charm Quark Production

Production of charm quark at LHC energies is dominated by gluon interactions of the colliding protons. In the following we discuss three examples of such processes: Gluonic pair production, gluon splitting and flavour excitation whose feynman diagrams are shown in Figure 1, Figure 2 and Figure 3.
Gluonic pair production is a hard process in which two gluons annihilate and form a $c\bar{c}$ pair in the final state. Gluon splitting is where two gluons undergo a hard scattering process that is followed by one gluon splitting into a $c\bar{c}$ pair. Flavour excitation is a process whereby a gluon from one proton splits into a $c\bar{c}$ pair that is then hard scattered by a gluon from the other proton. The cross sections of these processes can be calculated in pertubative QCD. However, the initial gluon distribution has to be known and is an input to such calculations.

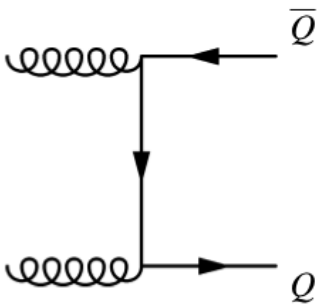

Figure 1: Gluonic pair production: In a hard process two gluons annihilate and form a $c\bar{c}$ pair in the final state. Diagram taken from ref. [27].

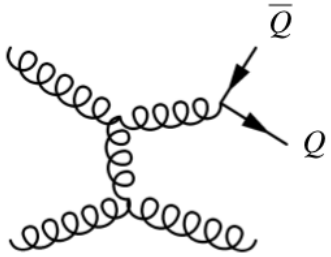

Figure 2: Gluon splitting: Two gluons undergo a hard scattering process that is followed by one gluon splitting into a $c\bar{c}$ pair. Diagram taken from ref. [27].

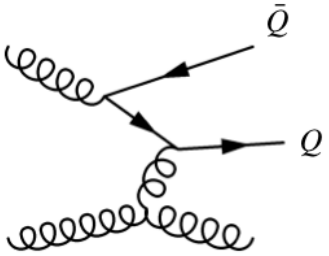

Figure 3: Flavour excitation: A gluon from one proton splits into a $c\bar{c}$ pair that is then hard scattered by a gluon from the other proton. Diagram taken from ref. [27].

2.2 Fragmentation

Experimentally, it has been observed that free quarks do not exist. According to the colour neutrality postulate in quantum chromodynamics, colour charged particles only occur in colour-neutral hadrons in nature. Therefore, the sole constituents of a produced $c\bar{c}$ pair in the LHC hadronise into hadrons soon after production. As the attracting force between two opposed colour-charged quarks remains constant with increasing distance, there is a linear increase of potential energy. Thus, if the distance between the quarks becomes large enough it is energetically favourable that a $q\bar{q}$ pair is produced from vaccum. In this way the charm quarks and antiquarks can find up and down quarks and antiquarks and combine to D mesons. The regarded types of D mesons are discussed in Section 2.3. The process of quarks hadronising into hadrons is also called fragmentation.
Fragmentation is a soft process and can therefore not be described in pertubative QCD calculations. For this reason it must be modelled by experimentally-determined fragmentation functions. Equation (2) shows a fragmentation function that C.Peterson et al. [26] formulated in 1983 on the basis of simple quantum mechanical considerations:

$$D_Q^H(z) \propto \frac{1}{z[1-(1/z)-\epsilon_Q/(1-z)]^2} \tag{1}$$

where $z = E_H/E_Q, E_Q$ is the energy of the incoming heavy quark and E_H is the energy of the outgoing hadron. ϵ_Q is defined as $\epsilon_Q = (m_q/m_Q)^2$ where m_q and m_Q are the masses of the light and heavy quarks. However, for calculation purposes ϵ_Q is taken to be a free a parameter.

2.3 Meson Species and Decay Channels

The focus in this thesis lays on the charmed mesons D^0, D^+ and D^{*+}. They consist of a c quark and a light antiquark: $\bar{u}$ for D^0, $\bar{d}$ for D^+ and D^{*+}. The fragmentation fraction (FF) is the relative production yield of a charm quark hadronizing to a particular species of D meson. They are assumed to be universal, i.e. they do not depend on the colliding system, the collision energy or the absolute quark energy. The values for D^0, D^+ and D^{*+} are provided by the Particle Data Group [18] are given in Equation (2). They have been measured at LEP at the Z-resonance [6, 17].

$$\begin{aligned} \mathrm{FF}_{c\to D^0} &= 0.557 \pm 0.023 \\ \mathrm{FF}_{c\to D^+} &= 0.226 \pm 0.010 \\ \mathrm{FF}_{c\to D^{*+}} &= 0.238 \pm 0.007 \end{aligned} \tag{2}$$

At the ALICE experiment the D mesons cannot be detected directly as their lifetimes are too short. Therefore, one exploits the hadronic decays:

$$\begin{aligned} D^0 &\to K^- + \pi^+ \\ D^+ &\to K^- + \pi^+ + \pi^+ \\ D^{*+} &\to D^0 + \pi^+ \end{aligned} \tag{3}$$

with branching ratios (BR) [18]:

$$\begin{aligned} \mathrm{BR}_{D^0\to K^-\pi^+} &= 3.89 \pm 0.05\% \\ \mathrm{BR}_{D^+\to K^-\pi^+\pi^+} &= 9.13 \pm 0.19\% \\ \mathrm{BR}_{D^{*+}\to D^0\pi^+} &= 67.7 \pm 0.5\% \end{aligned} \tag{4}$$

The branching ratios specify the possibiltiy for a particular D meson to decay into the specified channel. With the ALICE detector being capable of assigning the detected kaons and pions to original numbers of D^0, D^+ and D^{*+} it is possible to tell about the numbers of D^0, D^+ and D^{*+} that were produced in the fragmentation process.

2.4 FONLL

FONLL stands for Fixed Order plus Next Leading Logarithm. It is a pertubative QCD calculation framework that calculates differential cross sections for heavy quark production in hadron-hadron collisions [27]. In comparison to other pQCD frameworks such as MNR [23] it provides more accurate results for large p_{t}. The cross sections are calculated using the factorization Ansatz [27] according to

$$\mathrm{d}\sigma(\mathrm{pp} \to \mathrm{D} + X) = \sum_{i,j,k} \int \mathrm{d}x_1 \mathrm{d}x_2 \mathrm{d}z f_i(x_1, \mu_{\mathrm{F}}) f_j(x_2, \mu_{\mathrm{F}}) \times \mathrm{d}\sigma_{ij \to kX}(\mu_{\mathrm{F}}, \alpha_{\mathrm{S}}(\mu_{\mathrm{R}}, m_{\mathrm{k}}) D_k^D(z) \quad (5)$$

where i and j denote the interacting partons in the colliding protons and k the outgoing heavy quark with mass m_k.
f_i (f_j) is the parton distributing function (PDF) of the parton i (j). The PDF is a probability density for the parton i (j) carrying momentum fraction x_1 (x_2) within the colliding protons. The FONLL data used within this thesis used the CTEQ6.6 [24] PDF.
$\mathrm{d}\sigma_{ij \to kX}$ is the sum of differential cross sections of processes in which the incoming partons i and j interact and form the heavy quark k in the final state. The $\mathrm{d}\sigma_{ij \to kX}$ are calculated in pQCD.
μ_{F} and μ_{R} are the factorization and renormalization scales. They are an input to the PDFs and the differential cross sections calculated in pQCD. In general, the pQCD calculations suffer from divergencies leading to infinite results. To avoid these infinities, μ_{F} and μ_{R} are introduced. A complete calculation would not depend on the choice of these scales. However, in the absence of such complete calculation, the results do depend on the scale variables. To estimate the uncertainty introduced by these scales, one varies them up and down. See Section 3.4.2 for the exact procedure used within this thesis.
α_{S} is the strong coupling constant and m_k is the mass of the outgoing quark k.
$D_k^D(z)$ is the fragmentation function describing the probability of the outgoing quark k fragmenting to a D meson. See Section 2.2 for further discussion of this process.

The FONLL spectra used within this thesis come in two groups. One group are p_{t} differential cross section spectra for each D meson with a rapidity cutoff of $|y| < 0.5$. The other group are p_{t} differential cross section spectra for each D meson for the full rapidity range. These spectra are provided by Cacciari et al. [11] [12].

2.4.1 GM-VFNS and MNR

GM-VFNS and MNR are pQCD frameworks closely related to FONLL. The main diffrence between these frameworks lays in the handling of infinities.

In general, the pQCD calculations contain badly converging logarithmic terms at higher orders, especially when the relevant energy scale, e.g. the quark p_{t}, is much larger than the quark mass.

Resummation approaches such as FONLL and GM-VFNS share the goal of resumming leading and next-to-leading logarithmic (NLL) terms to all orders in the cross section. Once a massless but resummed result, valid in the $\mathrm{E} \gg \mathrm{m}$ region, is obtained, one makes the interpolation to a fixed order cross section, valid in the $\mathrm{E} \approx \mathrm{m}$ region, to arrive at a prediction over the whole E range. FONLL and GM-VFNS differ in the way this interpolation is realized, amongst others.

It turns out that this approach leads to an enhancement compared to MNR: The resulting heavy-quark hadron spectrum at high-pt is in better agreement with experimantally observed data, while the total heavy-quark production cross section dominated by the low pt part remains practically unchanged.

3 Methods

The aim of this thesis was to develop a program, that computes from the visible production cross sections of prompt (B feed-down subtracted) D mesons, both their total production cross sections and their production cross section per unit of rapidity, at mid-rapidity $|y| < 0.5$.
From the total production cross section of each D meson the total charm production cross section is computed by taking into account the mesons' fragmentation fractions.
Moreover, P_v, the fraction of $c\bar{d}$ mesons produced in a vector state is calculated.

3.1 Program design

The programing concept used is object-oriented. Two ROOT classes were written from scratch that provide datastructure and methods allowing for easy use and expansion. A macro that uses the classes specifies the input data to be used and the quantities to be calculated.

3.2 Terminology

- $\sigma^{D}_{vis.}$: The visible cross section of the prompt production of a D meson. Within this thesis it is also referred to as the visible production cross section of a prompt D meson.
- σ^{D}_{tot}: The total cross section of the prompt production of a D meson. Within this thesis it is also referred to as the total production cross section of a prompt D meson.
- $d\sigma^{D}/dy$: The production cross section of a D meson per unit of rapidity at mid-rapidity $|y| < 0.5$
- P_v: The fraction of $c\bar{d}$ mesons produced in a vector state.
- $\sigma^{tot}_{c\bar{c}}$: The total charm production cross section.

3.3 Visible production cross sections of D mesons

The $\sigma^{\mathrm{D}}_{\mathrm{vis.}}$ have been obtained from the measured p_{t} differential cross section spectra by integrating over the experimentally covered p_{t} ranges and are reported in Table 1. These spectra have been measured at the ALICE experiment at CERN for both $\sqrt{s} = 2.76\,\mathrm{TeV}$ and $\sqrt{s} = 7\,\mathrm{TeV}$. The experimentally covered rapidity range at ALICE is $|y| < 0.5$. Figure 4 shows the measured spectra for $\sqrt{s} = 2.76\,\mathrm{TeV}$ and the ratio of the measured cross section and the central FONLL [11, 12] and GM-VFNS [19–21] calculations. In case of $\sqrt{s} = 2.76\,\mathrm{TeV}$, the fraction of D mesons created within the evaluated p_{t}-ranges for $|y| < 0.5$ is about 75 % in case of D^0 and about 40 % in case of D^+ and D^{*+}. In case of $\sqrt{s} = 7\,\mathrm{TeV}$ with wider p_{t} ranges these fractions are all about 80 %. The p_{t} ranges are given in Table 1 for the evaluated p_{t} ranges along with the visible cross sections.

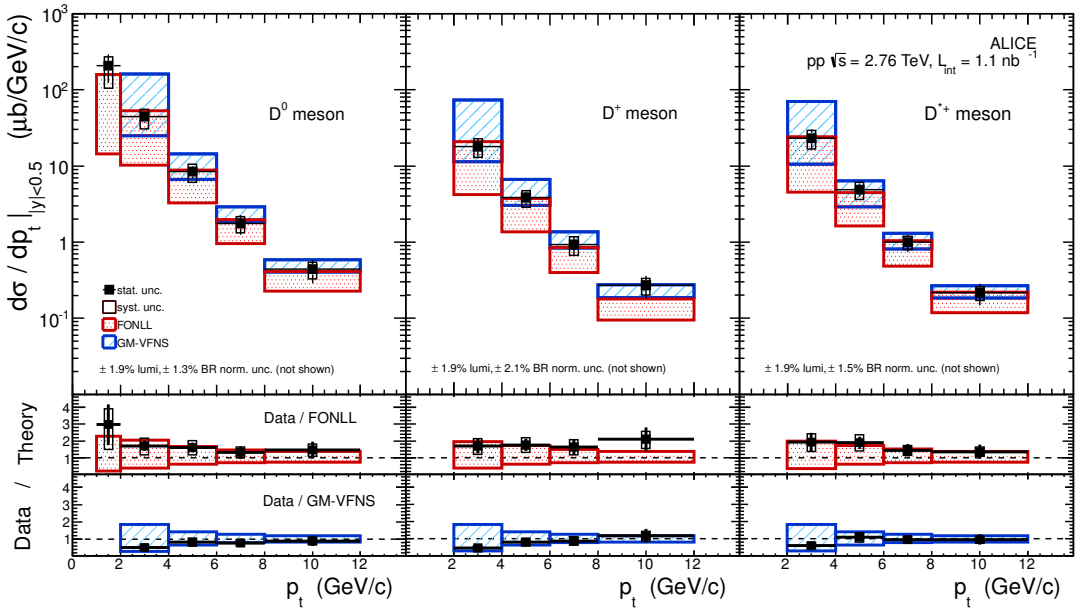

Figure 4: Top: p_{t}-differential cross section for prompt D^0, D^+, and D^{*+} mesons in pp collisions at $\sqrt{s} = 2.76$ TeV compared with FONLL [11,12] and GM-VFNS [19–21] theoretical predictions. Bottom: the ratio of the measured cross section and the central FONLL and GM-VFNS calculations. Plot taken from ref. [4]

Meson	$\sqrt{s}$ (TeV)	$p_{\rm t}$ interval (GeV/c)	$\sigma^{\rm D}_{\rm vis}\pm$ stat. $\pm$ syst. (μb)
$\rm D^0$	2.76	1–12	$317 \pm 85\ ^{+72}_{-120}$
$\rm D^+$	2.76	2–12	$47 \pm 9\ ^{+10}_{-12}$
$\rm D^{*+}$	2.76	2–12	$59 \pm 14\ ^{+13}_{-14}$
$\rm D^0$	7	1–16	$412 \pm 33\ ^{+55}_{-140}$
$\rm D^+$	7	1–24	$198 \pm 24\ ^{+42}_{-73}$
$\rm D^{*+}$	7	1–24	$203 \pm 23\ ^{+30}_{-67}$

Table 1: Visible production cross sections of prompt D mesons, $\sigma^{\rm D}_{\rm vis}(|y| < 0.5)$ in pp collisions at $\sqrt{s} = 2.76$ and 7 TeV. The normalization systematic uncertainty of 1.9% (3.5%) at $\sqrt{s} = 2.76$ (7) TeV and the decay BR uncertainties are not quoted here.

3.4 Production cross sections $\mathrm{d}\sigma^{\rm D}/\mathrm{d}y$ and total production cross sections $\sigma^{\rm D}_{\rm tot}$

3.4.1 Central values

The $\sigma^{\rm D}_{\rm tot}$ are computed by extrapolating the visible cross sections to the full phase space (full rapidity and $p_{\rm t}$ range). $\mathrm{d}\sigma^{\rm D}/\mathrm{d}y$ is computed by extrapolating the visible cross sections to the full $p_{\rm t}$ range.

$$\mathrm{d}\sigma^{\rm D}/\mathrm{d}y = \sigma^{\rm D}_{\rm vis.} \cdot f^{|y|<0.5}_{\rm FONLL} \tag{6}$$

$$\sigma^{\rm D}_{\rm tot} = \sigma^{\rm D}_{\rm vis.} \cdot f^{\text{all } y}_{\rm FONLL} \tag{7}$$

The extrapolation factors are computed from the FONLL $p_{\rm t}$-differential cross section spectra as the ratio between the spectra integrated over all $p_{\rm t}$ and the spectra

integrated over the measured p_t ranges:

$$f_\mathrm{FONLL}^{|y|<0.5} = \frac{\int_{\text{all } p_\mathrm{t}} \left(\frac{\mathrm{d}\sigma}{\mathrm{d}p_\mathrm{t}}\right)_{\text{FONLL, } |y|<0.5} \mathrm{d}p_\mathrm{t}}{\int_{p_\mathrm{t}\text{min.}}^{p_\mathrm{t}\text{max.}} \left(\frac{\mathrm{d}\sigma}{\mathrm{d}p_\mathrm{t}}\right)_{\text{FONLL, } |y|<0.5} \mathrm{d}p_\mathrm{t}} \tag{8}$$

$$f_\mathrm{FONLL}^{\text{all } y} = \frac{\int_{\text{all } p_\mathrm{t}} \left(\frac{\mathrm{d}\sigma}{\mathrm{d}p_\mathrm{t}}\right)_{\text{FONLL, all } y} \mathrm{d}p_\mathrm{t}}{\int_{p_\mathrm{t}\text{min.}}^{p_\mathrm{t}\text{max.}} \left(\frac{\mathrm{d}\sigma}{\mathrm{d}p_\mathrm{t}}\right)_{\text{FONLL, } |y|<0.5} \mathrm{d}p_\mathrm{t}} \tag{9}$$

This is a standard procedure for heavy quark cross section extrapolation.

3.4.2 Extrapolation uncertainties

As described in Section 2.4, the FONLL spectra come up with some uncertainties. To estimate the uncertainties of the f_FONLL arising from these uncertainties, there is a set of $f_\mathrm{FONLL,varied}$ calculated for each extrapolation factor f_FONLL. The disctinct $f_\mathrm{FONLL,varied}$ are calculated according to Equation (6) and Equation (7) where within the FONLL spectra used, μ_F, μ_R and m_c had been varied around their central values. The central values of both μ_F and μ_R are $m_\mathrm{t} = \sqrt{p_\mathrm{t}^2 + m_\mathrm{c}^2}$. μ_F and μ_R are varied in the ranges $0.5 \leq \mu_\mathrm{F}/m_\mathrm{t} \leq 2$ and $0.5 \leq \mu_\mathrm{R}/m_\mathrm{t} \leq 2$ with the constraint $0.5 \leq \mu_\mathrm{F}/\mu_\mathrm{R} \leq 2$. For the charm quark mass the central value is $m_\mathrm{c} = 1.5\,\mathrm{GeV/c^2}$. It is varied within $1.3 \leq m_\mathrm{c} \leq 1.7\,\mathrm{GeV/c^2}$. For the $\sqrt{s} = 7\,\mathrm{TeV}$ data there is also an up and down variation of the PDF performed. The obtained $f_\mathrm{FONLL,varied}$ are grouped into two (three) groups, depending on which kind of variation has been performed.:

- $\mu_\mathrm{F}, \mu_\mathrm{R}$
- m_c
- PDF (only for $\sqrt{s} = 7\,\mathrm{TeV}$)

Note that there is no $f_\mathrm{FONLL,varied}$ that is a member of more than one group. Within each group the largest positive and negative deviation of the $f_\mathrm{FONLL,varied}$ are determined and taken as the uncertainties correponding to the respective group. The total uncertainties of the f_FONLL are calculated as the quadratic sum of the uncertainties of the two (three) groups:

$$\Delta f_\mathrm{FONLL} = \sqrt{\Delta^2_{\mu_\mathrm{F},\mu_\mathrm{R}} + \Delta^2_{m_\mathrm{c}} + \Delta^2_\mathrm{PDF}} \tag{10}$$

The extrapolation uncertainties of $\mathrm{d}\sigma^{\mathrm{D}}/\mathrm{d}y$ and $\sigma^{\mathrm{D}}_{\mathrm{tot}}$ are calculated by scaling the uncertainties of the f_{FONLL}:

$$\Delta^{\mathrm{extr.}}(\mathrm{d}\sigma^{\mathrm{D}}/\mathrm{d}y) = \Delta(f^{|y|<0.5}_{\mathrm{FONLL}}) \cdot \sigma^{\mathrm{D}}_{\mathrm{vis.}} \tag{11}$$

$$\Delta^{\mathrm{extr.}}(\sigma^{\mathrm{D}}_{\mathrm{tot}}) = \Delta(f^{\mathrm{all}\ y}_{\mathrm{FONLL}}) \cdot \sigma^{\mathrm{D}}_{\mathrm{vis.}} \tag{12}$$

3.4.3 Other uncertainties

The luminosity uncertainties and branching ratio uncertainties of $\mathrm{d}\sigma^{\mathrm{D}}/\mathrm{d}y$ and $\sigma^{\mathrm{D}}_{\mathrm{tot}}$ are calculated by multiplying them with the relative uncertainties of the luminosity and the branching ratios. The relative luminosity uncertainties have been measured in a dedicated run in ALICE [25]. The relative branching ratio uncertainties are provided by the PDG [18]. See Appendix 6.1 for equations.
Statistical uncertainties and systematical uncertainties are computed by a scaling of the particular uncertainties of the $\sigma^{\mathrm{D}}_{\mathrm{vis.}}$. See Appendix 6.2 for equations.

3.5 $\mathrm{P_v}$

$\mathrm{P_v}$ is defined as the proportion of $\mathrm{c\bar{d}}$ D mesons produced in a vector state. It is calculated by taking the ratio of $\sigma_{\mathrm{tot}}(\mathrm{D}^{*+})$ to the sum of $\sigma_{\mathrm{tot}}(\mathrm{D}^{*+})$ and the part of $\sigma_{\mathrm{tot}}(\mathrm{D}^{+})$ not originating from $\sigma_{\mathrm{tot}}(\mathrm{D}^{*+})$ decays.:

$$\mathrm{P_v} = \frac{\sigma_{\mathrm{tot}}(\mathrm{D}^{*+})}{\sigma_{\mathrm{tot}}(\mathrm{D}^{*+}) + \sigma_{\mathrm{tot}}(\mathrm{D}^{+}) - \sigma_{\mathrm{tot}}(\mathrm{D}^{*+}) \cdot (1 - \mathrm{BR}_{\mathrm{D}^{*+}\to\mathrm{D}^0\pi^+})} \tag{13}$$

$$= \frac{\sigma_{\mathrm{tot}}(\mathrm{D}^{*+})}{\sigma_{\mathrm{tot}}(\mathrm{D}^{+}) + \sigma_{\mathrm{tot}}(\mathrm{D}^{*+}) \cdot \mathrm{BR}_{\mathrm{D}^{*+}\to\mathrm{D}^0\pi^+}} \tag{14}$$

3.5.1 Uncertainties

The statistical uncertainty and the systematical uncertainty of $\mathrm{P_v}$ are obtained from adding up quadratically the contributions of $\sigma_{\mathrm{tot}}(\mathrm{D}^{+})$ and $\sigma_{\mathrm{tot}}(\mathrm{D}^{*+})$. To be sure not to underestimate the systematical uncertainty of $\mathrm{P_v}$ and in order to keep things simple at the same time, the systematical uncertainties of $\sigma_{\mathrm{tot}}(\mathrm{D}^{+})$ and $\sigma_{\mathrm{tot}}(\mathrm{D}^{*+})$ are symmetrized using the larger of the absolutes of their upper and lower uncertainties before error propagation is performed. See Appendix 6.3 for equations.

The branching ratio uncertainty is evaluated summing in quadrature the uncertainties of the branching ratios as presented in Appendix 6.4.
Luminosity uncertainties cancel out as $\sigma_{\mathrm{tot}}(\mathrm{D}^+)$ and $\sigma_{\mathrm{tot}}(\mathrm{D}^{*+})$ scale identically to each other with a change in the luminosity.
The procedure for the calculation of the extrapolation uncertainty of $\mathrm{P_v}$ is identical to the one used for the f_{FONLL} described in Section 3.4.2. $\mathrm{P_v}$ is calculated for each variation of the FONLL input parameters and the largest positive and negative deviations of each group of variations are taken as the uncertainties corresponding to the respective group. These uncertainties are then summed up quadratically:

$$\Delta^{\mathrm{extr.}}(\mathrm{P_v}) = \sqrt{\Delta^2_{\mu_\mathrm{F},\mu_\mathrm{R}} + \Delta^2_{m_\mathrm{c}} + \Delta^2_{\mathrm{PDF}}} \tag{15}$$

3.6 Total charm production cross section $\sigma^{\mathrm{tot}}_{\mathrm{c\bar{c}}}$

The total charm production cross section $\sigma^{\mathrm{tot}}_{\mathrm{c\bar{c}}}$ is calculated as a weighted average of the total charm production cross section derived from $\sigma_{\mathrm{tot}}(\mathrm{D}^0)$ and $\sigma_{\mathrm{tot}}(\mathrm{D}^+)$, that is $\sigma^{\mathrm{tot}}_{\mathrm{c\bar{c}};\,\mathrm{D}^0,\mathrm{D}^+}$, and the total charm production cross section derived from $\sigma_{\mathrm{tot}}(\mathrm{D}^{*+})$, $\sigma^{\mathrm{tot}}_{\mathrm{c\bar{c}};\,\mathrm{D}^{*+}}$, using the inverse of the squared statistical uncertainties as weights.:

$$\sigma^{\mathrm{tot}}_{\mathrm{c\bar{c}}} = \underbrace{\frac{\frac{\sigma^{\mathrm{tot}}_{\mathrm{c\bar{c}};\,\mathrm{D}^0,\mathrm{D}^+}}{\left[\Delta^{\mathrm{stat.}}\left(\sigma^{\mathrm{tot}}_{\mathrm{c\bar{c}};\,\mathrm{D}^0,\mathrm{D}^+}\right)\right]^2} + \frac{\sigma^{\mathrm{tot}}_{\mathrm{c\bar{c}};\,\mathrm{D}^{*+}}}{\left[\Delta^{\mathrm{stat.}}\left(\sigma^{\mathrm{tot}}_{\mathrm{c\bar{c}};\,\mathrm{D}^{*+}}\right)\right]^2}}{\left[\Delta^{\mathrm{stat.}}\left(\sigma^{\mathrm{tot}}_{\mathrm{c\bar{c}};\,\mathrm{D}^0,\mathrm{D}^+}\right)\right]^{-2} + \left[\Delta^{\mathrm{stat.}}\left(\sigma^{\mathrm{tot}}_{\mathrm{c\bar{c}};\,\mathrm{D}^{*+}}\right)\right]^{-2}}}_{norm.} \tag{16}$$

3.6.1 Uncertainties

The statistical, fragmentation fraction and branching ratio uncertainties of $\sigma^{\mathrm{tot}}_{\mathrm{c\bar{c}}}$ are computed by adding up quadratically the contributions of $\sigma^{\mathrm{tot}}_{\mathrm{c\bar{c}};\,\mathrm{D}^0,\mathrm{D}^+}$ and $\sigma^{\mathrm{tot}}_{\mathrm{c\bar{c}};\,\mathrm{D}^{*+}}$.
The systematical uncertainty of $\sigma^{\mathrm{tot}}_{\mathrm{c\bar{c}}}$ is calculated by adding up linearly the contributions of $\sigma^{\mathrm{tot}}_{\mathrm{c\bar{c}};\,\mathrm{D}^0,\mathrm{D}^+}$ and $\sigma^{\mathrm{tot}}_{\mathrm{c\bar{c}};\,\mathrm{D}^{*+}}$.
The luminosity uncertainty of $\sigma^{\mathrm{tot}}_{\mathrm{c\bar{c}}}$ is calculated by multiplying $\sigma^{\mathrm{tot}}_{\mathrm{c\bar{c}}}$ with the relative luminosity uncertainty. See Appendices 6.5 to 6.8 for equations.
The procedure for the calculation of the extrapolation uncertainty of $\sigma^{\mathrm{tot}}_{\mathrm{c\bar{c}}}$ is identical to the one used for the f_{FONLL} described in Section 3.4.2. $\sigma^{\mathrm{tot}}_{\mathrm{c\bar{c}}}$ is calculated for each variation of the FONLL input parameters and the obtained uncertainties are summed up quadratically:

$$\Delta^{\mathrm{extr.}}(\sigma_{\mathrm{tot}}) = \sqrt{\Delta^2_{\mu_\mathrm{F},\mu_\mathrm{R}} + \Delta^2_{m_\mathrm{c}} + \Delta^2_{\mathrm{PDF}}} \tag{17}$$

3.7 Total charm production cross section $\sigma^{\mathrm{tot}}_{\mathrm{c\bar{c}};\,\mathrm{D^0,D^+}}$

The total charm production cross section derived from $\sigma_{\mathrm{tot}}(\mathrm{D}^0)$ and $\sigma_{\mathrm{tot}}(\mathrm{D}^+)$, $\sigma^{\mathrm{tot}}_{\mathrm{c\bar{c}};\,\mathrm{D^0,D^+}}$, is calculated by dividing the sum of $\sigma_{\mathrm{tot}}(\mathrm{D}^0)$ and $\sigma_{\mathrm{tot}}(\mathrm{D}^+)$ by the sum of the corresponding fragmentation fractions:

$$\sigma^{\mathrm{tot}}_{\mathrm{c\bar{c}};\,\mathrm{D^0,D^+}} = \frac{\sigma_{\mathrm{tot}}(\mathrm{D}^0) + \sigma_{\mathrm{tot}}(\mathrm{D}^+)}{\mathrm{FF}_{\mathrm{c}\to\mathrm{D}^0} + \mathrm{FF}_{\mathrm{c}\to\mathrm{D}^+}} \tag{18}$$

3.7.1 Uncertainties

The statistical, systematical and branching ratio uncertainties are calculated by a scaling of the quadratically summed up uncertainties of $\sigma_{\mathrm{tot}}(\mathrm{D}^0)$ and $\sigma_{\mathrm{tot}}(\mathrm{D}^+)$.
The luminosity uncertainty and the fragmentation fraction uncertainty are calculated by multiplying $\sigma^{\mathrm{tot}}_{\mathrm{c\bar{c}};\,\mathrm{D^0,D^+}}$ with the relative uncertainty of the luminosity and the relative uncertainty of the sum of the fragmentation fractions, respectivly. See Appendices 6.9 and 6.10 for equations.
The procedure for the calculation of the extrapolation uncertainty of $\sigma^{\mathrm{tot}}_{\mathrm{c\bar{c}};\,\mathrm{D^0,D^+}}$ is identical to the one used for the f_{FONLL} described in Section 3.4.2.
$\sigma^{\mathrm{tot}}_{\mathrm{c\bar{c}};\,\mathrm{D^0,D^+}}$ is calculated for each variation of the FONLL input parameters and the obtained uncertainties are summed up quadratically:

$$\Delta^{\mathrm{extr.}}(\sigma^{\mathrm{tot}}_{\mathrm{c\bar{c}};\,\mathrm{D^0,D^+}}) = \sqrt{\Delta^2_{\mu_{\mathrm{F}},\mu_{\mathrm{R}}} + \Delta^2_{m_{\mathrm{c}}} + \Delta^2_{\mathrm{PDF}}} \tag{19}$$

3.8 Total charm production cross section $\sigma^{\mathrm{tot}}_{\mathrm{c\bar{c}};\,\mathrm{D^{*+}}}$

The total charm production cross section derived from $\sigma_{\mathrm{tot}}(\mathrm{D}^{*+})$, $\sigma^{\mathrm{tot}}_{\mathrm{c\bar{c}};\,\mathrm{D}^{*+}}$, is calculated by dividing $\sigma_{\mathrm{tot}}(\mathrm{D}^{*+})$ by the corresponding fragmentation fraction.:

$$\sigma^{\mathrm{tot}}_{\mathrm{c\bar{c}};\,\mathrm{D}^{*+}} = \frac{\sigma_{\mathrm{tot}}(\mathrm{D}^{*+})}{\mathrm{FF}_{\mathrm{c}\to\mathrm{D}^{*+}}} \tag{20}$$

3.8.1 Uncertainies

The luminosity uncertainty and the fragmentation fraction uncertainty of $\sigma^{\mathrm{tot}}_{\mathrm{c\bar{c}};\,\mathrm{D}^{*+}}$ are calculated by multiplying $\sigma^{\mathrm{tot}}_{\mathrm{c\bar{c}};\,\mathrm{D}^{*+}}$ with the relative uncertainty of the luminosity and the relative uncertainty of the fragmentation fraction, respectivly. The statistical, systematical, branching ratio and extrapolation uncertainties are calculated from a scaling of the uncertainties of $\sigma_{\mathrm{tot}}(\mathrm{D}^{*+})$.
See Appendices 6.11 to 6.12 for equations.

4 Results

With the program developed within this thesis most numbers were reproduced. However, there were differnces in the error propagation. All diffrences could be identified as bugs in the old code.

4.1 Production cross sections $\mathrm{d}\sigma^{\mathrm{D}}/\mathrm{d}y$ and $\sigma^{\mathrm{D}}_{\mathrm{tot}}$

It turned out, that the lower extrapolation uncertainties of the differential cross sections per unit of rapidity for D^0, D^+ and D^{*+} in case of $\sqrt{s} = 7\,\mathrm{TeV}$ and D^0 in case of $\sqrt{s} = 2.76\,\mathrm{TeV}$ had been calculated 15-20 % too large by the old program due to implementation errors. More precisely, the part in the old code that is responsible for finding the largest positive and negative deviations within each group of the $f_{\mathrm{FONLL,varied}}$ does not distinguish properly between the groups. In effect, some of the $f_{\mathrm{FONLL,varied}}$ are taken into account twice what leads to too large uncertainties in the cases specied above.

Table 2 shows the production cross sections per unit of rapidity, $\mathrm{d}\sigma^{\mathrm{D}}/\mathrm{d}y$, of D mesons in μb, integrated over all p_{t} for $|y| < 0.5$. Numbers that were calculated wrongly by the old code are bold printed.

Meson	$\sqrt{s}$ (TeV)	$\mathrm{d}\sigma^{\mathrm{D}}/\mathrm{d}y$	stat.	syst.	lum.	BR	extr.
D^0	2.76	428	± 115	$^{+98}_{-163}$	± 8	± 6	$^{+151}_{\mathbf{-20}}$
D^+	2.76	127	± 26	$^{+28}_{-31}$	± 2	± 3	$^{+38}_{-23}$
D^{*+}	2.76	148	± 35	$^{+33}_{-36}$	± 3	± 2	$^{+42}_{-23}$
D^0	7	516	± 41	$^{+69}_{-175}$	± 18	± 7	$^{+120}_{\mathbf{-31}}$
D^+	7	248	± 30	$^{+52}_{-92}$	± 9	± 5	$^{+57}_{\mathbf{-15}}$
D^{*+}	7	247	± 27	$^{+36}_{-81}$	± 9	± 4	$^{+57}_{\mathbf{-14}}$

Table 2: Production cross sections $\mathrm{d}\sigma^{\mathrm{D}}/\mathrm{d}y$ (μb) of D mesons, integrated over all p_{t} for $|y| < 0.5$. Numbers that were calculated wrongly by the old code are bold printed.

Table 3 shows the total production cross sections $\sigma^{\mathrm{D}}_{\mathrm{tot}}$ of D mesons in mb, extrapolated to the full phase space. In case of the total production cross sections all numbers were calculated correctly.
Table 4 shows the related extrapolations factors.

Meson	$\sqrt{s}$ (TeV)	$\sigma^{\mathrm{D}}_{\mathrm{tot}}$	stat.	syst.	lum.	BR	extr.
D^0	2.76	3.13	± 0.84	$^{+0.71}_{-1.19}$	± 0.06	± 0.04	$^{+2.02}_{-0.14}$
D^+	2.76	0.93	± 0.19	$^{+0.20}_{-0.22}$	± 0.02	± 0.02	$^{+0.41}_{-0.09}$
D^{*+}	2.76	1.08	± 0.25	$^{+0.24}_{-0.26}$	± 0.02	± 0.02	$^{+0.51}_{-0.10}$
D^0	7	4.42	$\pm$ 0.35	$^{+0.59}_{-1.50}$	$\pm$ 0.15	$\pm$ 0.06	$^{+2.59}_{-0.19}$
D^+	7	2.12	$\pm$ 0.26	$^{+0.45}_{-0.78}$	$\pm$ 0.07	$\pm$ 0.04	$^{+1.23}_{-0.09}$
D^{*+}	7	2.11	$\pm$ 0.24	$^{+0.31}_{-0.70}$	$\pm$ 0.07	$\pm$ 0.03	$^{+1.24}_{-0.08}$

Table 3: Total production cross sections $\sigma^{\mathrm{D}}_{\mathrm{tot}}$(mb) of D mesons, extrapolated to the full phase space.

Meson	$\sqrt{s}$(TeV)	extr. factor $\mathrm{d}\sigma^{\mathrm{D}}/\mathrm{d}y$	extr. factor $\sigma^{\mathrm{D}}_{\mathrm{tot}}$
D^0	2.76	$1.35\ ^{+0.48}_{-0.06}$	$9.9\ ^{+6.3}_{-0.4}$
D^+	2.76	$2.72\ ^{+0.80}_{-0.49}$	$19.9\ ^{+8.8}_{-1.9}$
D^{*+}	2.76	$2.50\ ^{+0.72}_{-0.39}$	$18.2\ ^{+8.6}_{-1.7}$
D^0	7	$1.25\ ^{+0.29}_{-0.08}$	$10.7\ ^{+6.3}_{-0.5}$
D^+	7	$1.25\ ^{+0.29}_{-0.08}$	$10.7\ ^{+6.2}_{-0.5}$
D^{*+}	7	$1.21\ ^{+0.28}_{-0.07}$	$10.4\ ^{+6.1}_{-0.4}$

Table 4: With FONLL calculated extrapolation factors for $\mathrm{d}\sigma^{\mathrm{D}}/\mathrm{d}y$ ($|y| < 0.5$) and $\sigma^{\mathrm{D}}_{\mathrm{tot}}$.

4.2 P_v

The obtained values for P_v, the fraction of $c\bar{d}$ D mesons created in a vector state, at $\sqrt{s} = 2.76\,\text{TeV}$ and $\sqrt{s} = 7\,\text{TeV}$ are given in Equation (21) and Equation (22) with the values that changed bold printed :

$$P_v(2.76\ \text{TeV}) = 0.65 \pm 0.11\,(\text{stat.})\ \mathbf{\pm 0.13}\ (\text{syst.})\ \mathbf{\pm 0.01}\ (\text{BR})\ ^{+0.011}_{\mathbf{-0.004}}(\text{extr.}) \tag{21}$$

$$P_v(7\ \text{TeV}) = 0.59 \pm 0.06\,(\text{stat.})\ \mathbf{\pm 0.18}\ (\text{syst.})\ \mathbf{\pm 0.01}\ (\text{BR})\ ^{+0.005}_{\mathbf{-0.003}}(\text{extr.}) \tag{22}$$

Several uncertainties were found to be calculated in a wrong way in the existing code:

- The systematical uncertainty is calculated 38 % (56 %) too small in case of $\sqrt{s} = 2.76\,\text{TeV}$ ($\sqrt{s} = 7\,\text{TeV}$). The exact procedure in the existing code could not be comprehended.
- The branching ratio uncertainty is calculated 80 % too small for both energies. There were several attempts made to identify the procedure used in the exsiting code. This included the implementation of a method that tries all possible combinations of propagating the branching ratio uncertainties within the calculation of P_v. However, the values produced by the old code could not be reproduced.
- The lower extrapolation uncertainty is calculated 35 % (49 %) too small in case of $\sqrt{s} = 2.76\,\text{TeV}$ ($\sqrt{s} = 7\,\text{TeV}$). Most likely, there is a bug in the part of the existing code, that is responsible for finding the largest positive and negative deviations within each group of calculated $P_{v,\,\text{varied}}$, similar to the bug in the calculation of the lower extrapolation factors of $d\sigma^D/dy$. However, this was not verified.

It is observed, that the extrapolation uncertainties of P_v are negligible what indicates, that the FONLL extrapolation factors of D^+ and D^{*+} scale almost identically to each other with the varying of the FONLL parameters.

The values are compatible with results from other experiments using diffrent colliding systems at diffrent collision energies, [2,3,5,7,10,14,16], as shown in Figure 5. The weighted average of the experimental measurements reported in ref. [15], with average 0.594 ± 0.010, and of the LHC data [2, 3, 5] shown in Figure 5 is $P_v = 0.60 \pm 0.01$, and is represented by a solid yellow vertical band in the figure. It is observed that the value of Pv is independent of the collision system and collision energy. In hindsight, this justifies the factorization Ansatz in Equation (5), which assumes that the creation of a charm quark and its hadronization are independent.

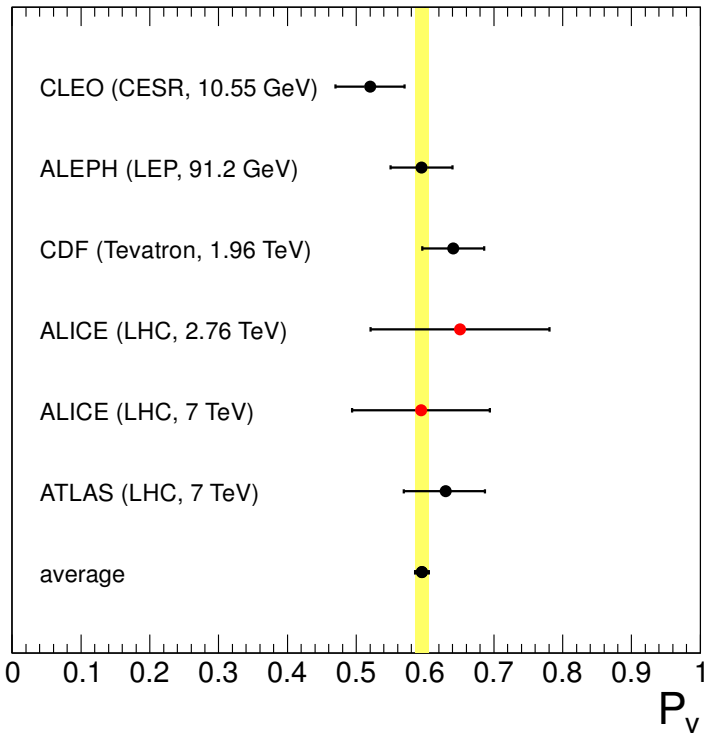

Figure 5: The fraction P_v of $c\bar{d}$ D mesons created in a vector state to vector and pseudoscalar prompt D mesons [2, 3, 5, 7, 10, 14, 16]. The weighted average of the experimental measurements reported in ref. [15] and of the LHC data [2,3,5] shown in the figure is $P_v = 0.60 \pm 0.01$, and is represented by a solid yellow vertical band. Plot taken from ref. [4].

4.3 Total charm production cross section

The total charm production cross section was taken as the weighed average of the total charm production cross section derived by the sum of the total production cross sections of D^0 and D^+ and the total charm production cross section derived by the total production cross section of D^{*+}:

$$\sigma^{\text{tot}}_{c\bar{c}} = \underbrace{\frac{\frac{\sigma^{\text{tot}}_{c\bar{c};\,D^0,D^+}}{\left[\Delta^{\text{stat.}}\left(\sigma^{\text{tot}}_{c\bar{c};\,D^0,D^+}\right)\right]^2} + \frac{\sigma^{\text{tot}}_{c\bar{c};\,D^{*+}}}{\left[\Delta^{\text{stat.}}\left(\sigma^{\text{tot}}_{c\bar{c};\,D^{*+}}\right)\right]^2}}{\left[\Delta^{\text{stat.}}\left(\sigma^{\text{tot}}_{c\bar{c};\,D^0,D^+}\right)\right]^{-2} + \left[\Delta^{\text{stat.}}\left(\sigma^{\text{tot}}_{c\bar{c};\,D^{*+}}\right)\right]^{-2}}}_{norm.} \tag{23}$$

See Sections 3.7 and 3.8 for further information.

Table 5 shows total charm production cross sections in mb. Values that were calculated according to a wrong procedure in the old code are in bold print.

$\sqrt{s}$ (TeV)	$\sigma^{\text{tot}}_{c\bar{c}}$	stat.	syst.	BR	FF.	lum.	extr.
2.76	4.8	0.8	$^{+1.0}_{-1.3}$	**0.06**	0.1	**0.1**	$\mathbf{^{+2.6}_{-0.4}}$
7	8.5	0.5	$^{+1.0}_{-2.4}$	**0.09**	0.2	**0.3**	$\mathbf{^{+5.0}_{-0.4}}$

Table 5: Calculated total charm production cross sections. The bold printed rows show the weighted averages of $\sigma^{\text{tot}}_{c\bar{c};\,D^0,D^+}$ and $\sigma^{\text{tot}}_{c\bar{c};\,D^{*+}}$.

Some of the uncertainties calculated by the existing code were found to be incorrect:

- The branching ratio uncertainty was calculated 30 % too small in case of $\sqrt{s} = 2.76\,\text{TeV}$. In case of $\sqrt{s} = 7\,\text{TeV}$ a change does not appear in the given precision. In the old code, the contributions of the branching ratio uncertanties of $\sigma^{\text{tot}}_{c\bar{c};\,D^0,D^+}$ and $\sigma^{\text{tot}}_{c\bar{c};\,D^{*+}}$ are summed up in quadrature. This is wrong as both $\sigma^{\text{tot}}_{c\bar{c};\,D^0,D^+}$ and $\sigma^{\text{tot}}_{c\bar{c};\,D^{*+}}$ depend on $\text{BR}_{D^0\to K^-\pi^+}$.
- The luminosity uncertainties were both calculated about 20 % too small. In the old code, the contributions of the luminosity uncertainties of $\sigma^{\text{tot}}_{c\bar{c};\,D^0,D^+}$ and $\sigma^{\text{tot}}_{c\bar{c};\,D^{*+}}$ are summed up in quadrature. This is wrong as $\sigma^{\text{tot}}_{c\bar{c};\,D^0,D^+}$ and $\sigma^{\text{tot}}_{c\bar{c};\,D^{*+}}$ scale identically to each other with a change in the luminosity.
- The upper extrapolation uncertainty in case of $\sqrt{s} = 2.76\,\text{TeV}$ was calculated 8 % too small. The lower extrapolation uncertainty in case of $\sqrt{s} = 2.76\,\text{TeV}$ and both lower and upper extrapolation uncertainties in case of $\sqrt{s} = 7\,\text{TeV}$

were calculated about 20 % too small. In the old code, the extrapolation uncertainty of $\sigma^{\mathrm{tot}}_{\mathrm{c\bar{c}};\,\mathrm{D^0,D^+}}$ is calculated from summing up in quadrature the contributions of $\sigma_{\mathrm{tot}}(\mathrm{D^0})$ and $\sigma_{\mathrm{tot}}(\mathrm{D^+})$. This is wrong as they are correlated. This wrongly calculated extrapolation uncertainty of $\sigma^{\mathrm{tot}}_{\mathrm{c\bar{c}};\,\mathrm{D^0,D^+}}$ is then used to calculate the extrapolation uncertainty of $\sigma^{\mathrm{tot}}_{\mathrm{c\bar{c}}}$ which is therefore incorrect.

Figure 6 shows the total nucleon–nucleon charm production cross section [1–3, 8, 9, 22] as a function of the collision energy. The uncertainty boxes around the ATLAS [2, 3] and ALICE [5] points denote the extrapolation uncertainties alone, whilst the uncertainty bars are the overall uncertainties. Note that in case of proton–nucleus (pA) or deuteron–nucleus (dA) collisions, the measured cross sections have been scaled down by the number of binary nucleon–nucleon collisions calculated in a Glauber model of the proton–nucleus or the deuteron–nucleus collision geometry. At $\sqrt{s} = 7$ TeV, the ALICE results are in agreement with preliminary measurements by the ATLAS [2, 3] and the LHCb Collaboration [1]. The curves show the calculations at next-to-leading-order within the MNR framework [23] together with its uncertainties using the same parameters (and parameter uncertainties) mentioned before for FONLL. The overall dependence on the collision energy is described by pQCD calculations.

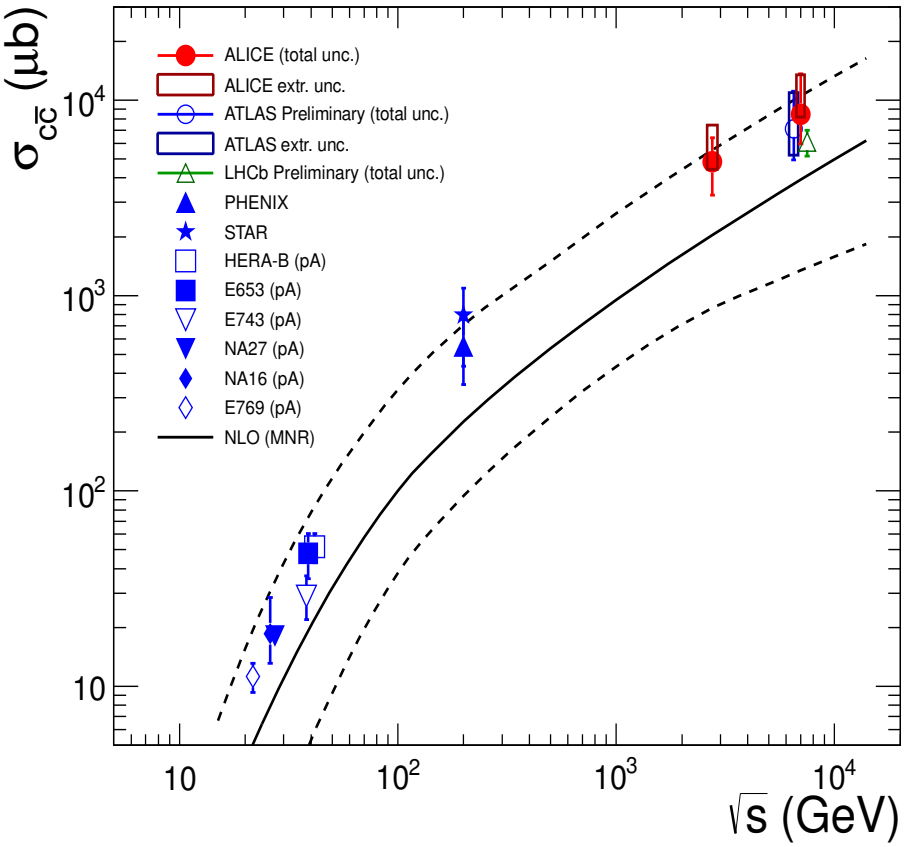

Figure 6: Energy dependence of the total nucleon–nucleon charm production cross section [1–3, 8, 9, 22]. In case of proton–nucleus (pA) or deuteron–nucleus (dA) collisions, the measured cross sections have been scaled down by the number of binary nucleon–nucleon collisions calculated in a Glauber model of the proton–nucleus or deuteron–nucleus collision geometry. The NLO MNR calculation [23] (and its uncertainties) is represented by solid (dashed) lines. Plot taken from ref. [4].

4.4 D_s^+

The program was originally designed for the three mesons D^0, D^+ and D^{*+}. After having thoroughly checked that all methods worked correctly and after all discrepancies found between the values produced by my code and the values produced by the old code were understood, I added the D_s^+ meson. This implementation process took only about ten minutes which proves the easy maintenance of the developed code par exellence.

4.4.1 Data

The visible cross section of prompt D_s^+ mesons in proton-proton collisions at $\sqrt{s} = 7\,\text{TeV}$ was obtained from the p_t-differential cross section spectrum that was measured at ALICE and is shown in Figure 7. The symbols are positioned horizontally at the centre of each p_t interval. The normalization uncertainty (3.5 % from the minimum-bias cross section and 4.9 % from the branching ratio uncertainties) is not shown. Theoretical prediction from GM-VFNS [21] is also shown.

The visible cross section was obtained by integrating over the experimentally covered p_t range of $2 < p_t < 12$ and is given in Equation (24).

$$\sigma_{\text{vis.}}^{D_s^+} = 52 \pm 12\,(\text{stat.})\,^{+12}_{-15}\,(\text{syst.}) \pm 2\,(\text{lum.}) \pm 3\,(\text{BR})\,\mu\text{b} \tag{24}$$

As there are no FONLL predictions for the production of D_s^+ mesons at full rapidity so far, the visible cross section of D_s^+ is extrapolated only to the full p_t range. The production cross section of prompt D_s^+ mesons per unit of rapidity at midrapidity $|y| < 0.5$ is given in Equation (25):

$$\mathrm{d}\sigma^{D_s^+}\,\mathrm{d}y = 116 \pm 27\,(\text{stat.})\,^{+27}_{-34}\,(\text{syst.}) \pm 4\,(\text{lum.}) \pm 7\,(\text{BR})\,^{+36}_{-28}\,(\text{extr.})\,\mu\text{b} \tag{25}$$

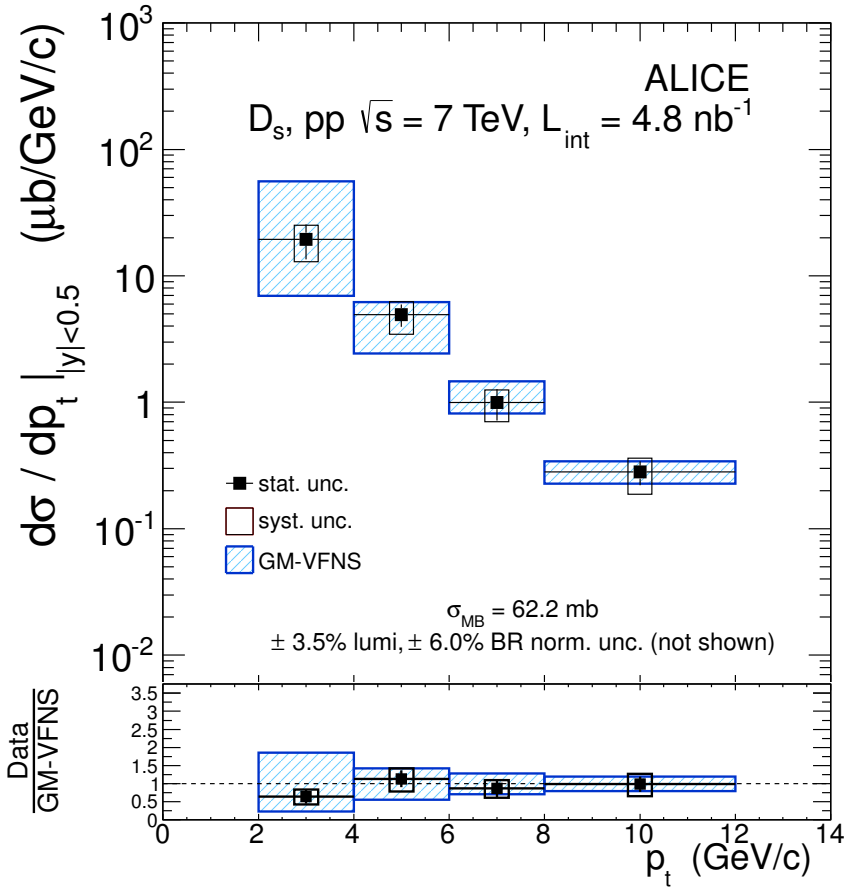

Figure 7: (colour online) p_{t}-differential inclusive cross section for prompt $\mathrm{D_s^+}$ mesons in proton-proton collisions at $\sqrt{s} = 7\,\mathrm{TeV}$. The symbols are positioned horizontally at the centre of each p_{t} interval. The normalization uncertainty (3.5 % from the minimum-bias cross section and 4.9 % from the branching ratio uncertainties) is not shown. Theoretical prediction from GM-VFNS [21] is also shown. Plot taken from ref. [13].

5 Summary

Within this thesis, a program was developed that extrapolates the measured, visible cross sections of D mesons to the full kinematical phase space. This had become necessary since the already existing program that was used for these extrapolations so far had become difficult to maintain.
In the process of comparing the values produced by the new program with the values produced by the existing program many bugs in the existing program could be identified. With the help of the developed program several values in the paper 'Measurement of charm production at central rapidity in proton-proton collisions at $\sqrt{s} = 2.76\,\mathrm{TeV}$' [4], that was being proofread whilst this thesis was written, could be corrected.
The within short time completed implementation of the $\mathrm{D_s^+}$ meson was interpreted as a first, passed test for the developed program.
As a first step of what can still be done to finalize the developed program, a method was implemented that calculates the visible cross section for a D meson by integrating over its p_t differential cross section spectrum. However, the read-in of the systematical uncertainties could not be finished.

6 Appendix

6.1 Luminosity uncertainties and branching ratio uncertainties of $\mathrm{d}\sigma^{\mathrm{D}}/\mathrm{d}y$ and $\sigma^{\mathrm{D}}_{\mathrm{tot}}$

The luminosity uncertainties and branching ratio uncertainties of $\mathrm{d}\sigma^{\mathrm{D}}/\mathrm{d}y$ and $\sigma^{\mathrm{D}}_{\mathrm{tot}}$ are calculated by multiplying them with the relative uncertainties of the luminosity and the branching ratios as :

- **luminosity uncertainties:**

$$\Delta^{\mathrm{lum.}}(\mathrm{d}\sigma^{\mathrm{D}}/\mathrm{d}y) = \mathrm{d}\sigma^{\mathrm{D}}/\mathrm{d}y \cdot \frac{\Delta L}{L} \tag{26}$$

$$\Delta^{\mathrm{lum.}}(\sigma^{\mathrm{D}}_{\mathrm{tot}}) = \sigma^{\mathrm{D}}_{\mathrm{tot}} \cdot \frac{\Delta L}{L} \tag{27}$$

- **branching ratio uncertainties:**

$$\Delta^{\mathrm{BR}}(\mathrm{d}\sigma^{\mathrm{D}}/\mathrm{d}y) = \mathrm{d}\sigma^{\mathrm{D}}/\mathrm{d}y \cdot \frac{\Delta \mathrm{BR}^{\mathrm{D}}}{\mathrm{BR}^{\mathrm{D}}} \tag{28}$$

$$\Delta^{\mathrm{BR}}(\sigma^{\mathrm{D}}_{\mathrm{tot}}) = \sigma^{\mathrm{D}}_{\mathrm{tot}} \cdot \frac{\Delta \mathrm{BR}^{\mathrm{D}}}{\mathrm{BR}^{\mathrm{D}}} \tag{29}$$

6.2 Statistical uncertainties and systematical uncertainties of $\mathrm{d}\sigma^{\mathrm{D}}/\mathrm{d}y$ and $\sigma^{\mathrm{D}}_{\mathrm{tot}}$

The statistical uncertainties and systematical uncertainties are computed by a scaling of the particular uncertainties of the $\sigma^{\mathrm{D}}_{\mathrm{vis.}}$.

- **statistical uncertainties:**

$$\Delta^{\mathrm{stat.}}(\mathrm{d}\sigma^{\mathrm{D}}/\mathrm{d}y) = \Delta^{\mathrm{stat.}}(\sigma^{\mathrm{D}}_{\mathrm{vis.}}) \cdot f^{|y|<0.5}_{\mathrm{FONLL}} \tag{30}$$

$$\Delta^{\mathrm{stat.}}(\sigma^{\mathrm{D}}_{\mathrm{tot}}) = \Delta^{\mathrm{stat.}}(\sigma^{\mathrm{D}}_{\mathrm{vis.}}) \cdot f^{\mathrm{all}\ y}_{\mathrm{FONLL}} \tag{31}$$

- **systematical uncertainties:**

$$\Delta^{\mathrm{syst.}}(\mathrm{d}\sigma^{\mathrm{D}}/\mathrm{d}y) = \Delta^{\mathrm{syst.}}(\sigma^{\mathrm{D}}_{\mathrm{vis.}}) \cdot f^{|y|<0.5}_{\mathrm{FONLL}} \tag{32}$$

$$\Delta^{\mathrm{syst.}}(\sigma^{\mathrm{D}}_{\mathrm{tot}}) = \Delta^{\mathrm{syst.}}(\sigma^{\mathrm{D}}_{\mathrm{vis.}}) \cdot f^{\mathrm{all}\ y}_{\mathrm{FONLL}} \tag{33}$$

6.3 Statistical uncertainty and systematical uncertainty of $\mathrm{P_v}$

The statistical uncertainty and the systematical uncertainty of $\mathrm{P_v}$ is obtained from gaussian error propagation:

$$\Delta(\mathrm{P_v}) = \left[\left(\frac{\partial \mathrm{P_v}}{\partial \sigma_{\mathrm{tot}}(\mathrm{D}^+)} \cdot \Delta(\sigma_{\mathrm{tot}}(\mathrm{D}^+)) \right)^2 + \left(\frac{\partial \mathrm{P_v}}{\partial \sigma_{\mathrm{tot}}(\mathrm{D}^{*+})} \cdot \Delta(\sigma_{\mathrm{tot}}(\mathrm{D}^{*+})) \right)^2 \right]^{\frac{1}{2}} \quad (34)$$

- **statistical uncertainty**

$$\Delta^{\mathrm{stat.}}(\mathrm{P_v}) = \mathrm{P_v^2} \cdot \left[\left(\frac{\sigma_{\mathrm{tot}}(\mathrm{D}^+)}{\sigma_{\mathrm{tot}}(\mathrm{D}^{*+})^2} \cdot \Delta^{\mathrm{stat.}}(\sigma_{\mathrm{tot}}(\mathrm{D}^{*+})) \right)^2 + \left(\frac{\Delta^{\mathrm{stat.}}(\sigma_{\mathrm{tot}}(\mathrm{D}^+))}{\sigma_{\mathrm{tot}}(\mathrm{D}^{*+})} \right)^2 \right]^{\frac{1}{2}} \quad (35)$$

- **systematical uncertainty**

$$\Delta^{\mathrm{syst.}}(\mathrm{P_v}) = \mathrm{P_v^2} \cdot \left[\left(\frac{\sigma_{\mathrm{tot}}(\mathrm{D}^+)}{\sigma_{\mathrm{tot}}(\mathrm{D}^{*+})^2} \cdot \Delta^{\mathrm{syst.}}(\sigma_{\mathrm{tot}}(\mathrm{D}^{*+})) \right)^2 + \left(\frac{\Delta^{\mathrm{syst.}}(\sigma_{\mathrm{tot}}(\mathrm{D}^+))}{\sigma_{\mathrm{tot}}(\mathrm{D}^{*+})} \right)^2 \right]^{\frac{1}{2}} \quad (36)$$

Note, that to guarantee not to underestimate the systematical uncertainty of $\mathrm{P_v}$ and in order to keep things simple at the same time, the systematical uncertainties of $\sigma_{\mathrm{tot}}(\mathrm{D}^+)$ and $\sigma_{\mathrm{tot}}(\mathrm{D}^{*+})$ are symmetrized using the larger of the absolutes of their upper and lower uncertainties before error propagation is performed.

6.4 Branching ratio uncertainty of $\mathrm{P_v}$

Equation (14) can be reformulated into:

$$\mathrm{P_v} = \frac{\left(\frac{N^*}{\mathrm{BR}_{\mathrm{D}^{*+} \to \mathrm{D}^0 \pi^+} \cdot \mathrm{BR}_{\mathrm{D}^0 \to \mathrm{K}^- \pi^+}} \right)}{\left(\sigma_{\mathrm{tot}}(\mathrm{D}^+) + \frac{N^*}{\mathrm{BR}_{\mathrm{D}^0 \to \mathrm{K}^- \pi^+}} \right)} \quad (37)$$

Gaussian error propagation leads to:

$$\Delta^{\mathrm{BR}}(\mathrm{P_v}) = \Bigg[\left(\frac{\mathrm{P_v}}{\mathrm{BR}_{\mathrm{D}^{*+}\to\mathrm{D}^0\pi^+}} \, \Delta\mathrm{BR}_{\mathrm{D}^{*+}\to\mathrm{D}^0\pi^+} \right)^2 + \left(\frac{\mathrm{P_v^2}}{\sigma_{\mathrm{tot}}(\mathrm{D}^{*+})} \Delta^{\mathrm{BR}}(\sigma_{\mathrm{tot}}(\mathrm{D}^+)) \right)^2 + \left(\frac{\mathrm{P_v^2} \; \sigma_{\mathrm{tot}}(\mathrm{D}^+)}{\sigma_{\mathrm{tot}}(\mathrm{D}^{*+}) \; \mathrm{BR}_{\mathrm{D}^0\to\mathrm{K}^-\pi^+}} \Delta\mathrm{BR}_{\mathrm{D}^0\to\mathrm{K}^-\pi^+} \right)^2 \Bigg]^{\frac{1}{2}} \tag{38}$$

6.5 Statistical uncertainty and fragmentatin fraction uncertainty of $\sigma^{\mathrm{tot}}_{\mathrm{c\bar{c}}}$

The statistical and fragmentation fraction uncertainties of $\sigma^{\mathrm{tot}}_{\mathrm{c\bar{c}}}$ are computed by adding up quadratically the contributions of $\sigma^{\mathrm{tot}}_{\mathrm{c\bar{c}};\,\mathrm{D}^0,\mathrm{D}^+}$ and $\sigma^{\mathrm{tot}}_{\mathrm{c\bar{c}};\,\mathrm{D}^{*+}}$:

- **statistical uncertainty**

$$\Delta^{\mathrm{stat.}}\left(\sigma^{\mathrm{tot}}_{\mathrm{c\bar{c}}}\right) = \frac{1}{norm.} \times \left[\left(\frac{1}{\Delta^{\mathrm{stat.}}(\sigma^{\mathrm{tot}}_{\mathrm{c\bar{c}};\,\mathrm{D}^0,\mathrm{D}^+})} \right)^2 + \left(\frac{1}{\Delta^{\mathrm{stat.}}(\sigma^{\mathrm{tot}}_{\mathrm{c\bar{c}};\,\mathrm{D}^{*+}})} \right)^2 \right]^{\frac{1}{2}} \tag{39}$$

- **fragmentation fraction uncertainty**

$$\Delta^{\mathrm{FF.}}(\sigma^{\mathrm{tot}}_{\mathrm{c\bar{c}}}) = \frac{1}{norm.} \times \left[\left(\frac{\Delta^{\mathrm{FF.}}(\sigma^{\mathrm{tot}}_{\mathrm{c\bar{c}};\,\mathrm{D}^0,\mathrm{D}^+})}{\left[\Delta^{\mathrm{stat.}}(\sigma^{\mathrm{tot}}_{\mathrm{c\bar{c}};\,\mathrm{D}^0,\mathrm{D}^+})\right]^2} \right)^2 + \left(\frac{\Delta^{\mathrm{FF.}}(\sigma^{\mathrm{tot}}_{\mathrm{c\bar{c}};\,\mathrm{D}^{*+}})}{\left[\Delta^{\mathrm{stat.}}(\sigma^{\mathrm{tot}}_{\mathrm{c\bar{c}};\,\mathrm{D}^{*+}})\right]^2} \right)^2 \right]^{\frac{1}{2}} \tag{40}$$

6.6 Branching ratio uncertainty of $\sigma^{\mathrm{tot}}_{\mathrm{c\bar{c}}}$

To be able to perform error propagation of uncorrelated quantities, eq. (23) is reformulated into:

$$\sigma^{\mathrm{tot}}_{\mathrm{c\bar{c}}} = \left[\frac{\frac{N^0}{\mathrm{BR}_{\mathrm{D^0}\to\mathrm{K^-}\pi^+}} + \sigma_{\mathrm{tot}}(\mathrm{D^+})}{\left[\Delta^{\mathrm{stat.}}\left(\sigma^{\mathrm{tot}}_{\mathrm{c\bar{c}};\,\mathrm{D^0,D^+}}\right)\right]^2 (\mathrm{FF}_{\mathrm{c}\to\mathrm{D^0}} + \mathrm{FF}_{\mathrm{c}\to\mathrm{D^+}})} + \frac{N^*}{\left[\Delta^{\mathrm{stat.}}\left(\sigma^{\mathrm{tot}}_{\mathrm{c\bar{c}};\,\mathrm{D^{*+}}}\right)\right]^2 \mathrm{BR}_{\mathrm{D^{*+}}\to\mathrm{D^0}\pi^+}\mathrm{BR}_{\mathrm{D^0}\to\mathrm{K^-}\pi^+}\mathrm{FF}_{\mathrm{c}\to\mathrm{D^{*+}}}} \right] \times \frac{1}{norm.} \tag{41}$$

The branching ratio uncertainty of $\sigma^{\mathrm{tot}}_{\mathrm{c\bar{c}}}$ is calculated according to Equation (42):

$$\Delta^{\mathrm{BR}}\left(\sigma^{\mathrm{tot}}_{\mathrm{c\bar{c}}}\right) = \left[\left(\left[\frac{\mathrm{D^0}}{\left[\Delta^{\mathrm{stat.}}\left(\sigma^{\mathrm{tot}}_{\mathrm{c\bar{c}};\,\mathrm{D^0,D^+}}\right)\right]^2 (\mathrm{FF}_{\mathrm{c}\to\mathrm{D^0}} + \mathrm{FF}_{\mathrm{c}\to\mathrm{D^+}})} + \frac{\mathrm{D^{*+}}}{\left[\Delta^{\mathrm{stat.}}\left(\sigma^{\mathrm{tot}}_{\mathrm{c\bar{c}};\,\mathrm{D^{*+}}}\right)\right]^2 \mathrm{FF}_{\mathrm{c}\to\mathrm{D^{*+}}}} \right] \frac{\Delta\mathrm{BR}_{\mathrm{D^0}\to\mathrm{K^-}\pi^+}}{\mathrm{BR}_{\mathrm{D^0}\to\mathrm{K^-}\pi^+}} \right)^2 + \left(\frac{\Delta^{\mathrm{BR}}(\sigma_{\mathrm{tot}}(\mathrm{D^+}))}{\left[\Delta^{\mathrm{stat.}}\left(\sigma^{\mathrm{tot}}_{\mathrm{c\bar{c}};\,\mathrm{D^0,D^+}}\right)\right]^2 (\mathrm{FF}_{\mathrm{c}\to\mathrm{D^0}} + \mathrm{FF}_{\mathrm{c}\to\mathrm{D^+}})} \right)^2 + \left(\frac{\mathrm{D^{*+}} \cdot \Delta\mathrm{BR}_{\mathrm{D^{*+}}\to\mathrm{D^0}\pi^+}}{\left[\Delta^{\mathrm{stat.}}\left(\sigma^{\mathrm{tot}}_{\mathrm{c\bar{c}};\,\mathrm{D^{*+}}}\right)\right]^2 \mathrm{FF}_{\mathrm{c}\to\mathrm{D^{*+}}} \cdot \mathrm{BR}_{\mathrm{D^{*+}}\to\mathrm{D^0}\pi^+}} \right)^2 \right]^{\frac{1}{2}} \times \frac{1}{norm.} \tag{42}$$

6.7 Systematical uncertainty of $\sigma^{\mathrm{tot}}_{\mathrm{c\bar{c}}}$

The systematical uncertainty of $\sigma^{\mathrm{tot}}_{\mathrm{c\bar{c}}}$ is calculated by adding up linearly the contributions of $\sigma^{\mathrm{tot}}_{\mathrm{c\bar{c}};\,\mathrm{D^0,D^+}}$ and $\sigma^{\mathrm{tot}}_{\mathrm{c\bar{c}};\,\mathrm{D^{*+}}}$.:

$$\Delta^{\mathrm{syst.}}\left(\sigma^{\mathrm{tot}}_{\mathrm{c\bar{c}}}\right) = \frac{1}{norm.} \times \left(\frac{\Delta^{\mathrm{syst.}}(\sigma^{\mathrm{tot}}_{\mathrm{c\bar{c}};\,\mathrm{D^0,D^+}})}{\left[\Delta^{\mathrm{stat.}}(\sigma^{\mathrm{tot}}_{\mathrm{c\bar{c}};\,\mathrm{D^0,D^+}})\right]^2} + \frac{\Delta^{\mathrm{syst.}}(\sigma^{\mathrm{tot}}_{\mathrm{c\bar{c}};\,\mathrm{D^{*+}}})}{\left[\Delta^{\mathrm{stat.}}(\sigma^{\mathrm{tot}}_{\mathrm{c\bar{c}};\,\mathrm{D^{*+}}})\right]^2} \right) \tag{43}$$

6.8 Luminosity uncertainty of $\sigma^{\mathrm{tot}}_{\mathrm{c\bar{c}}}$

The luminosity uncertainty of $\sigma^{\mathrm{tot}}_{\mathrm{c\bar{c}}}$ is calculated by multiplying $\sigma^{\mathrm{tot}}_{\mathrm{c\bar{c}}}$ with the relative luminosity uncertainty:

$$\Delta^{\mathrm{lum.}}(\sigma^{\mathrm{tot}}_{\mathrm{c\bar{c}}}) = \frac{\Delta L}{L} \cdot \sigma^{\mathrm{tot}}_{\mathrm{c\bar{c}}} \tag{44}$$

6.9 Statistical, systematical and branching ratio uncertainties of $\sigma^{\mathrm{tot}}_{\mathrm{c\bar{c}};\,\mathrm{D^0,D^+}}$

The statistical, systematical and branching ratio uncertainties are calculated by a scaling of the quadratically summed up uncertainties of $\sigma_{\mathrm{tot}}(\mathrm{D^0})$ and $\sigma_{\mathrm{tot}}(\mathrm{D^+})$.:

- **statistical uncertainty**

$$\Delta^{\mathrm{stat.}}(\sigma^{\mathrm{tot}}_{\mathrm{c\bar{c}};\,\mathrm{D^0,D^+}}) = \frac{\sqrt{\Delta^{\mathrm{stat.}}(\sigma_{\mathrm{tot}}(\mathrm{D^0}))^2 + \Delta^{\mathrm{stat.}}(\sigma_{\mathrm{tot}}(\mathrm{D^+}))^2}}{\mathrm{FF}_{\mathrm{c\to D^0}} + \mathrm{FF}_{\mathrm{c\to D^+}}} \tag{45}$$

- **systematical uncertainty**

$$\Delta^{\mathrm{syst.}}(\sigma^{\mathrm{tot}}_{\mathrm{c\bar{c}};\,\mathrm{D^{*+}}}) = \frac{\sqrt{\Delta^{\mathrm{syst.}}(\sigma_{\mathrm{tot}}(\mathrm{D^0}))^2 + \Delta^{\mathrm{syst.}}(\sigma_{\mathrm{tot}}(\mathrm{D^+}))^2}}{\mathrm{FF}_{\mathrm{c\to D^0}} + \mathrm{FF}_{\mathrm{c\to D^+}}} \tag{46}$$

- **branching ratio uncertainty**

$$\Delta^{\mathrm{BR}}(\sigma^{\mathrm{tot}}_{\mathrm{c\bar{c}};\,\mathrm{D^{*+}}}) = \frac{\sqrt{\Delta^{\mathrm{BR}}(\sigma_{\mathrm{tot}}(\mathrm{D^0}))^2 + \Delta^{\mathrm{BR}}(\sigma_{\mathrm{tot}}(\mathrm{D^+}))^2}}{\mathrm{FF}_{\mathrm{c\to D^0}} + \mathrm{FF}_{\mathrm{c\to D^+}}} \tag{47}$$

6.10 Luminosity uncertainty and fragmentation fraction uncertainty of $\sigma^{\mathrm{tot}}_{\mathrm{c\bar{c}};\,\mathrm{D^0,D^+}}$

The luminosity uncertainty and the fragmentation fraction uncertainty are calculated by multiplying $\sigma^{\mathrm{tot}}_{\mathrm{c\bar{c}};\,\mathrm{D^0,D^+}}$ with the relative uncertainty of the luminosity and the the relative uncertainty of the sum of the fragmentation fractions, respectivly.

- **luminosity uncertainty**

$$\Delta^{\mathrm{lum.}}(\sigma^{\mathrm{tot}}_{\mathrm{c\bar{c}};\,\mathrm{D^0,D^+}}) = \frac{\Delta L}{L} \cdot \sigma^{\mathrm{tot}}_{\mathrm{c\bar{c}};\,\mathrm{D^0,D^+}} \tag{48}$$

- **fragmentation fraction**

$$\Delta^{\mathrm{FF.}}(\sigma^{\mathrm{tot}}_{\mathrm{c\bar{c}};\,\mathrm{D^0,D^+}}) = \sigma^{\mathrm{tot}}_{\mathrm{c\bar{c}};\,\mathrm{D^0,D^+}} \cdot \frac{\sqrt{(\Delta \mathrm{FF}_{\mathrm{c}\to\mathrm{D^0}})^2 + (\Delta \mathrm{FF}^2_{\mathrm{c}\to\mathrm{D^+}})}}{\mathrm{FF}_{\mathrm{c}\to\mathrm{D^0}} + \mathrm{FF}_{\mathrm{c}\to\mathrm{D^+}}} \tag{49}$$

6.11 Luminosity uncertainty and fragmentation fraction uncertainty of $\sigma^{\mathrm{tot}}_{\mathrm{c\bar{c}};\,\mathrm{D^{*}+}}$

The luminosity uncertainty and the fragmentation fraction uncertainty are calculated by multiplying $\sigma^{\mathrm{tot}}_{\mathrm{c\bar{c}};\,\mathrm{D^{*}+}}$ with the relative uncertainty of the luminosity and the relative uncertainty of the fragmentation fraction, respectivly.

- **luminosity uncertainty**

$$\Delta^{\mathrm{lum.}}(\sigma^{\mathrm{tot}}_{\mathrm{c\bar{c}};\,\mathrm{D^{*}+}}) = \frac{\Delta L}{L} \cdot \sigma^{\mathrm{tot}}_{\mathrm{c\bar{c}};\,\mathrm{D^{*}+}} \tag{50}$$

- **fragmentation fraction**

$$\Delta^{\mathrm{FF.}}(\sigma^{\mathrm{tot}}_{\mathrm{c\bar{c}};\,\mathrm{D^{*}+}}) = \sigma^{\mathrm{tot}}_{\mathrm{c\bar{c}};\,\mathrm{D^{*}+}} \cdot \frac{\Delta \mathrm{FF}_{\mathrm{c}\to\mathrm{D^{*}+}}}{\mathrm{FF}_{\mathrm{c}\to\mathrm{D^{*}+}}} \tag{51}$$

6.12 Other uncertainties of $\sigma^{\mathrm{tot}}_{\mathrm{c\bar{c}};\,\mathrm{D^{*}+}}$

All other uncertainties are computed from a scaling of the uncertainties of $\sigma^{\mathrm{tot}}_{\mathrm{c\bar{c}};\,\mathrm{D^{*}+}}$:

- **statistical uncertainty**

$$\Delta^{\text{stat.}}(\sigma^{\text{tot}}_{\text{c}\bar{\text{c}};\,\text{D}^{*+}}) = \frac{\Delta^{\text{stat.}}(\sigma_{\text{tot}}(\text{D}^{*+}))}{\text{FF}_{\text{c}\to\text{D}^{*+}}} \tag{52}$$

- **systematical uncertainty**

$$\Delta^{\text{syst.}}(\sigma^{\text{tot}}_{\text{c}\bar{\text{c}};\,\text{D}^{*+}}) = \frac{\Delta^{\text{syst.}}(\sigma_{\text{tot}}(\text{D}^{*+}))}{\text{FF}_{\text{c}\to\text{D}^{*+}}} \tag{53}$$

- **branching ratio uncertainty**

$$\Delta^{\text{BR}}(\sigma^{\text{tot}}_{\text{c}\bar{\text{c}};\,\text{D}^{*+}}) = \frac{\Delta^{\text{BR}}(\sigma_{\text{tot}}(\text{D}^{*+}))}{\text{FF}_{\text{c}\to\text{D}^{*+}}} \tag{54}$$

- **extraction uncertainty**

$$\Delta^{\text{extr.}}(\sigma^{\text{tot}}_{\text{c}\bar{\text{c}};\,\text{D}^{*+}}) = \frac{\Delta^{\text{extr.}}(\sigma_{\text{tot}}(\text{D}^{*+}))}{\text{FF}_{\text{c}\to\text{D}^{*+}}} \tag{55}$$

7 References

[1] Prompt charm production in *pp* collisions at $\sqrt{s} = 7$ TeV. Technical Report LHCb-CONF-2010-013, CERN, Geneva, Dec 2010.

[2] Comparison of D* meson production cross sections with FONLL and GM-VFNS predictions. Technical Report ATL-PHYS-PUB-2011-012, CERN, Geneva, 2011.

[3] Measurement of D* meson production cross sections in pp collisions at $\sqrt{s} =$ 7 TeV with the ATLAS detector. Technical Report ATLAS-CONF-2011-017, CERN, Geneva, Mar 2011.

[4] Measurement of charm production at central rapidity in proton proton collisions at sqrt {s}= 2.76 TeV. Technical Report CERN-PH-EP-2012-133, CERN, Geneva, 2012.

[5] B. Abelev, A. Abrahantes Quintana, D. Adamová, AM Adare, MM Aggarwal, G. Aglieri Rinella, AG Agocs, A. Agostinelli, S. Aguilar Salazar, Z. Ahammed, et al. Measurement of charm production at central rapidity in proton-proton collisions at $\sqrt{s} = 7$ TeV. *Journal of High Energy Physics*, 2012(1):1–30, 2012.

[6] K. Ackerstaff et al. Measurement of f(c -> D*+ X), f(b -> D*+ X) and $\gamma_{c\bar{c}}/\gamma_{had}$ using D*+/- mesons. *Eur.Phys.J.*, C1:439–459, 1998.

[7] D. Acosta. Measurement of prompt charm meson production cross sections in $p\overline{p}$ collisions at $\sqrt{s} = 1.96$ TeV. *Phys. Rev. Lett.*, 91:241804, Dec 2003.

[8] L. Adamczyk et al. Measurements of D^0 and D^* Production in $p+p$ Collisions at $\sqrt{s} = 200$ GeV. *Phys.Rev.*, D85:092010, 2012.

[9] A. Adare, S. Afanasiev, C. Aidala, NN Ajitanand, Y. Akiba, H. Al-Bataineh, J. Alexander, A. Al-Jamel, K. Aoki, L. Aphecetche, et al. Heavy-quark production in p+p and energy loss and flow of heavy quarks in au+ au collisions at sqrt [s_ {NN}]= 200 gev. *Physical Review C*, 84(4):044905, 2011.

[10] R. Barate. Study of charm production in Z decays. *The European Physical Journal C-Particles and Fields*, 16(4):597–611, 2000.

[11] M. Cacciari, S. Frixione, N. Houdeau, M.L. Mangano, P. Nason, and G. Ridolfi. Theoretical predictions for charm and bottom production at the LHC. *Arxiv preprint arXiv:1205.6344*, 2012.

[12] M. Cacciari, M. Greco, and P. Nason. The pt spectrum in heavy-flavour hadro-production. *Journal of High Energy Physics*, 1998:007, 1998.

[13] ALICE Collaboration. D_s^+ meson prodution at central rapidity in proton-proton collisions at $\sqrt{s}$ =7 TeV. unpublished.

[14] CDF collaboration. Blessed plots for 'measurement of the direct charm meson production cross section at CDF. http://www-cdf.fnal.gov/physics/new/bottom/030403.blessed-dxsec/. CDF Note 6623.

[15] A. David. Is the fragmentation of charm quarks into D mesons described by heavy quark effective theory? *Physics Letters B*, 644(4):224–227, 2007.

[16] M.C. de la Barca Sánchez. Open charm production from d+Au collisions in STAR. *The European Physical Journal C-Particles and Fields*, 43(1):187–192, 2005.

[17] Leonid Gladilin. Charm hadron production fractions, 1999. hep-ex/9912064.

[18] Particle Data Group et al. K. nakamura, et. al. *J. Phys. G: Nucl. Part. Phys*, 37:075021, 2010.

[19] B.A. Kniehl, G. Kramer, I. Schienbein, and H. Spiesberger. Collinear subtractions in hadroproduction of heavy quarks. *The European Physical Journal C-Particles and Fields*, 41(2):199–212, 2005.

[20] B.A. Kniehl, G. Kramer, I. Schienbein, and H. Spiesberger. Hadroproduction of D and B mesons in a massive VFNS. *AIP Conf.Proc.*, 792:867–870, 2005.

[21] B.A. Kniehl, G. Kramer, I. Schienbein, and H. Spiesberger. Inclusive Charmed-Meson Production at the CERN LHC. 2012.

[22] C. Lourenco and H.K. Wohri. Heavy flavour hadro-production from fixed-target to collider energies. *Phys.Rept.*, 433:127–180, 2006.

[23] M.L. Mangano, P. Nason, and G. Ridolfi. Heavy-quark correlations in hadron collisions at next-to-leading order. *Nuclear Physics B*, 373(2):295–345, 1992.

[24] Pavel M. Nadolsky, Hung-Liang Lai, Qing-Hong Cao, Joey Huston, Jon Pumplin, et al. Implications of CTEQ global analysis for collider observables. *Phys.Rev.*, D78:013004, 2008.

[25] K. Oyama. Cross-section normalization in proton–proton collisions at 2.76 and 7 tev, with ALICE at the LHC. *Journal of Physics G: Nuclear and Particle Physics*, 38:124131, 2011.

[26] C. Peterson, D. Schlatter, I. Schmitt, and P.M. Zerwas. Scaling violations in inclusive e^{+} e^{-} annihilation spectra. *Physical Review D*, 27(1):105, 1983.

[27] J. Wilkinson. Analysis and extrapolation of D meson cross sections at the LHC, 2011. Bachelor thesis, University of Heidelberg, unpublished.

Acknowledgment

Many thanks go to my supervisor Dr. Kai Schweda, who motivated me to write my bachelor thesis in the field of heavy quark production. His constant assistance and also his guidance while I was working on my bachelor thesis, motivated and helped me a lot.

...Thanks go to Dipl. Phys. Robert Grajcarek and Dipl. Phys. Daniel Lohner for all their advice and help in programing issues.

...Thanks go to Felix Florian Friedrich Frey for all the inspiring discussions I have had with him.

...Finally I want to thank the total group for the pleasant atmosphere.

This work has been supported by the Federal Ministry of Education and Research under promotional reference 06HD197D and by HA216/EMMI.

Declaration

I declare that I have written this thesis independently and that I have used no other than the specified sources and resources.

Heidelberg, August 7, 2012

.....
Stephan Stiefelmaier